Journal of Molecular Biology, **395**, 357-389 (2010) http://www.ncbi.nlm.nih.gov/pubmed/19883658

Insights into Cleavage Specificity from the Crystal Structure of Foot-and-Mouth Disease Virus 3C Protease Complexed with a Peptide Substrate

Patricia A. Zunszain[1], Stephen R. Knox[2], Trevor R. Sweeney[1], Jingjie Yang[1], Núria Roqué-Rosell[2], Graham J. Belsham[3], Robin J. Leatherbarrow[2] and Stephen Curry[1]*

[1]Biophysics Section, Blackett Laboratory, Imperial College, Exhibition Road, London, SW7 2AZ, UK.

[2]Department of Chemistry, Imperial College, Exhibition Road, London, SW7 2AZ, UK.

[3]Technical University of Denmark, National Veterinary Institute, Lindholm, 4771 Kalvehave, Denmark.

**Corresponding author: Email: s.curry@imperial.ac.uk; Tel: +44-20-7594-7632; Fax: +44-20-7589-0191*

doi:10.1016/j.jmb.2009.10.048

Picornavirus replication is critically dependent on the correct processing of a polyprotein precursor by the 3C protease at multiple, specific sites with related but non-identical sequences. To investigate the structural basis of its cleavage specificity, we performed the first crystallographic structural analysis of non-covalent complexes of a picornavirus 3C protease with peptide substrates. The X-ray crystal structure of the foot-and-mouth disease virus 3C protease (FMDV 3C^{pro}), mutated to replace the catalytic Cys by Ala, bound to a peptide (APAKQ|LLNFD) corresponding to the P5-P5′ region of the VP1-2A cleavage junction in the viral polyprotein was determined to 2.5 Å resolution. Comparison with the free enzyme reveals significant conformational changes in 3C^{pro} on substrate binding that lead to formation of an extended interface of contact primarily involving the P4-P2′ positions of the peptide. Strikingly, the deep S1′ specificity pocket needed to accommodate P1′-Leu only forms when the peptide binds. The substrate specificity was investigated using peptide-cleavage assays to show the impact of amino acid substitutions within the P5-P4′ region of synthetic substrates. The structure of the enzyme-peptide complex explains both the marked substrate preferences for particular P4, P2 and P1 residue types as well as the relative promiscuity at P3 and on the P′ side of scissile bond. Further, crystallographic analysis of the complex with a modified VP1-2A peptide (APAKE|LLNFD), containing a Gln to Glu substitution, reveals an identical mode of peptide binding and explains the ability of FMDV 3C^{pro} to cleave sequences containing either P1-Gln or P1-Glu. Structure-based mutagenesis was used to probe interactions within the S1′ specificity pocket and to provide direct evidence of the important contribution to proteolytic activity made by Asp 84 of the Cys-His-Asp catalytic triad. Our results provide a new level of detail in our understanding of the structural basis of polyprotein cleavage by 3C^{pro}.

Introduction

Foot-and-mouth disease (FMD) is a serious, widespread viral disease of cloven-hoofed animals, including important agricultural species such as cattle, sheep, pigs and goats[1,2]. The virus spreads rapidly and, although endemic and epidemic situations can be controlled using vaccines that are based on inactivated virus particles, political and technical difficulties with the maintenance and use of vaccine stocks has stimulated the search for alternative means of tackling the disease, such as anti-viral drugs[3]. The development of such treatments will demand a detailed knowledge of the molecular basis of viral replication. In this paper we focus on the structural basis of the cleavage activity of FMDV 3C^{pro}. As a highly conserved viral enzyme[4], FMDV 3C^{pro} is a potential drug target.

Foot–and-mouth disease virus (FMDV) is a single-stranded, positive sense RNA virus belonging to the picornavirus family that also includes human pathogens such as poliovirus (PV), human rhinovirus (HRV) and hepatitis A virus (HAV). Picornaviruses share a common replication strategy in which the viral RNA genome is translated in the cytoplasm of infected cells as a long polyprotein precursor that is cleaved by virally encoded proteases to release the functional proteins needed for synthesis of new virions. In all cases, the 3C protease (3C^{pro}) performs the majority of these cleavages (ten out of thirteen for FMDV) by targeting specific sequences within the polyprotein[2,5,6].

Structural studies on picornaviral 3C proteases revealed an overall fold that closely resembles the architecture of trypsin-like serine proteases[7-11]. The peptide-binding cleft, which contains the active site at its centre, is located at the interface between two β-barrels. Unusually, picornaviral 3C proteases possess a Cys-His-Asp/Glu catalytic triad at the centre of this cleft instead of the Ser-His-Asp arrangement of active site residues that is commonly found in serine proteases[12-14].

Most work to investigate the cleavage specificity of picornaviral 3C proteases has relied on extensive sequence analyses of the cleavage junctions within the polyprotein[3,15] or *in vitro* cleavage assays using protein or peptide substrates[8,16-20]. There is a surprising degree of variability in the sequences of the polyprotein junctions that are cleaved by picornaviral 3C proteases but these studies have nevertheless been valuable in identifying residues in the substrate that are important determinants of cleavage. Most picornavirus 3C proteases cleave the peptide bond between a highly conserved P1-Gln/P1´-Gly pair[15,21] [where P1 and P1´ denote the first amino acids on the N-terminal and C-terminal sides of the scissile bond respectively; in this notation[22] the corresponding sub-sites on the enzyme are labelled S1 and S1´]. FMDV 3C^{pro} is an interesting exception to this general pattern since it exhibits a preference either for substrates in which P1-Gln is followed by a relatively large, apolar amino acid in the P1´ position, or for P1Glu/P1´Gly junctions[3]. HAV 3C^{pro} can also tolerate larger P1´ amino acids in substrates with P1-Gln[21]. Other positions in the peptide also contribute to substrate recognition; in general there is a preference for a hydrophobic residue at P4 [16,18,19] and the nature of the P2 and P2´ amino acids, which vary between different picornavirus families, can also be important[8].

Extensive structural analysis of trypsin-like serine proteases have revealed a common mode of substrate binding in which the polypeptide sequence recognised by the enzyme lies in an extended conformation, similar to a β-strand, within the peptide binding cleft[23]. These enzymes typically recognise the alternating positions of the side chains along the sequence that are characteristic of an extended backbone conformation and this serves to place the scissile bond in the correct orientation at the active site. The primary specificity determinants in trypsin-like serine proteases are commonly located within the P4-P1 sequence[24-26] but can extend well beyond this core region for enzymes that are highly specific[27]. Crystallographic analysis of enzyme-substrate complexes reveals that viral 3C-like proteases, such as Tobacco Etch Virus NIa protease (TEV^{pro})[28] or the Severe Acute Respiratory Syndrome Coronavirus Main protease (SARS 3CL^{pro})[29], fall into the latter group since contacts with the enzyme can involve up to five or six amino acids on either side of the cleavage site. However, although both these proteases are '3C-like' in structure and have the common trypsin-like fold, they exhibit substantial differences from one another and from genuine picornaviral 3C proteases, especially in the loops that define the peptide-binding surface.

Previous structural analyses of picornavirus 3C^{pro}-peptide complexes have used relatively short, *covalently* attached peptides or peptide-mimicking inhibitors. In most cases the inhibitors were designed to bind to the S4-S1 sub-sites[24-26], though there is one report of the structure of an inhibitor bound to the S1´-S2´ sub-sites[30]. These studies are a powerful complement to cleavage assays since they have helped to elucidate the structural basis of amino acid recognition by these enzymes, particularly on the N-terminal side of the scissile bond. However, these studies cannot give a complete picture of protease-substrate interactions since in each case the peptide is covalently attached to the protease and represents at most one half of the peptide substrate that is recognised by the enzyme.

Here we report the first crystallographic analysis of a picornaviral 3C^{pro} complexed with an intact peptide substrate that spans P5-P5´. Our structural analysis of FMDV 3C^{pro} is combined with peptide cleavage assays that have examined the effect on specificity of amino acid variations within P5-P4´ and of mutations in the peptide-binding cleft of the enzyme. This concerted investigation provides a detailed and insightful description of the interactions between enzyme and substrate.

TABLE 1: Data collection and refinement statistics

DIFFRACTION DATA		
Peptide complex	*VP1-2A*	*VP1-2Am*
Synchrotron	*ESRF ID23-2*	*ESRF ID14-2*
Space-group	*$P2_12_12_1$*	*$P2_1$*
a, b, c (Å)	*64.8, 75,3, 86.0*	*64.0, 75.1, 86.3*
α, β, γ (°)	*90, 90, 90*	*90, 99.3, 90*
Resolution range (Å)[1]	*30.3 - 2.5 (2.66-2.5)*	*63.2- 2.7 (2.87-2.7)*
Independent reflections	*14044*	*16981*
Multiplicity[2]	*4.4 (2.5)*	*2.4 (2.6)*
Completeness (%)	*93.4 (78.5)*	*76.1 (60.8)*
I/σ_I	*9.1 (2.5)*	*8.6 (3.2)*
R_{merge} (%)	*13.9 (34.9)*	*8.6 (38.6)*
MODEL REFINEMENT		
Nonhydrogen atoms: protein/waters	*2958/33*	*6044/52*
R_{cryst} (%)	*21.2*	*23.6*
R_{free} (%)	*26.7*	*29.1*
r.m.s bond lengths (Å)	*0.008*	*0.008*
r.m.s bond angles (°)	*1.29*	*1.33*
Average B-factor (Å^2)	*46.7*	*32.1*
Ramachandran plot (% favoured/allowed)	*87.2/10.5*	*85.1/14.3*
PBD ID	*2wv4*	*2wv4*

[1]Resolution ranges for the highest resolution shells given in parentheses. [2]Values for the outermost resolution shell given in parentheses.

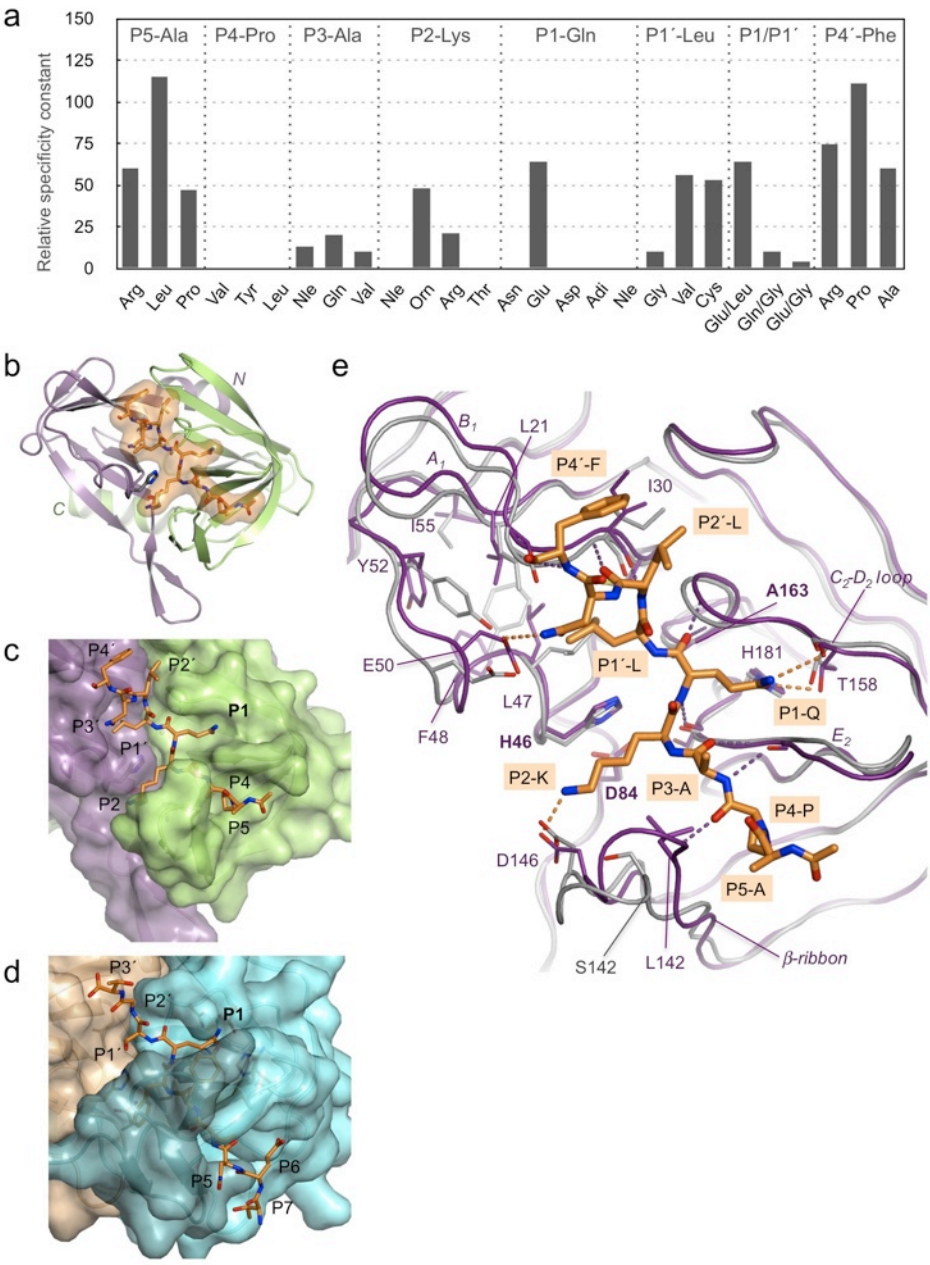

Figure 1: Overview of peptide recognition by FMDV 3C^{pro}. (a) Relative cleavage activity of FMDV 3C^{pro} against variants of the FRET4 substrate with amino acid substitutions in positions P5 to P4′. The activity is normalised with respect to the cleavage rate observed with wild-type substrate (Materials and Methods). The amino acids in the wild-type sequence are given at the top of each section; the identity of the substituted amino acid is given along the bottom. Note that in the P1/P1′ panel the Glu/Leu and Gln/Gly data bars are for single P1 and P1′ mutants respectively, but are duplicated here for ease of comparison with the Glu/Gly double mutant. (b) Schematic view of the co-crystal structure of 3C^{pro} (with N- and C-terminal β-barrels coloured lilac and green respectively) complexed with the VP1-2A peptide. The peptide is depicted in sticks colour-coded by atom type (carbon – orange; oxygen – red; nitrogen - blue) with its Van der Waals surface shown as a semi-transparent surface. (c) Surface representation of FMDV 3C^{pro} complexed with the VP1-2A peptide (sticks), coloured as in panel b. (d) Surface representation of TEV NIa 3C-like protease complexed with a P7-P3′peptide [28]. The N- and C-terminal β-barrels are coloured cyan and tan respectively). (e) Superposition of the free (grey) and peptide-bound (purple) forms of FDMV 3C^{pro}. The viewpoint is similar to that of panel b. Backbone-backbone hydrogen bonds are shown as purple dashed lines; other hydrogen bonds are coloured orange. Selected side chains are shown as sticks; secondary structural features that show greatest movement on peptide binding are labelled. Note that the unbound structure of FMDV 3C^{pro} has a Ser at position 142 (ref. 12).

Most strikingly we find that significant conformational adaptation by the enzyme is important for substrate recognition. This helps to explain several important aspects of specificity differences between the 3C proteases from different picornaviruses.

Results

Peptide cleavage assays

In conjunction with our structural analysis we performed an extensive investigation of the impact of sequence variation in the peptide on the rate of cleavage by FMDV 3C^{pro}. For these assays we synthesised a series of variants of FRET4, a modified peptide based on the P5-P8′ region of the VP1-2A cleavage junction[31], one of the ten sites cleaved by FMDV 3C^{pro} in the viral polyprotein. Cleavage of FRET4 produces a readily detectable increase in fluorescence[31] (Materials and Methods). The FRET4 variants, which contained single amino acid substitutions at positions P5-P1′ and P4′, or a double-substitution at P1 and P1′, were used in cleavage assays to determine the relative value of the specificity constant (k_{cat}/K_M) in each case (Fig. 1a).

A detailed account of the results of these experiments will be presented alongside the description of the structural features of peptide-protease interactions at each position along the substrate sequence (see below). Overall it is notable that—within the context of the VP1-2A sequence—variation at *all* positions from P4 to P1′ inclusive can reduce the rate of peptide cleavage by FMDV 3C^{pro} to between 0 and 50% of the rate observed with the control peptide (Fig. 1a). In contrast, variation at the P5 and P4′ positions at the extremities of the peptide had little impact on peptide cleavage. With one exception, these results are consistent with previous alanine-scanning analysis of the peptide[8]. They confirm the importance of positions P4, P2, P1 and P1′ for substrate recognition but reveal—for example—that residues at the P3 position can also contribute to cleavage specificity. The only inconsistency noted is that substitution of P4′-Phe (by Arg, Pro or Ala) had little effect on peptide cleavage in the fluorescence assay whereas previously it had been found in a HPLC-based assay that substitution by Ala abrogated

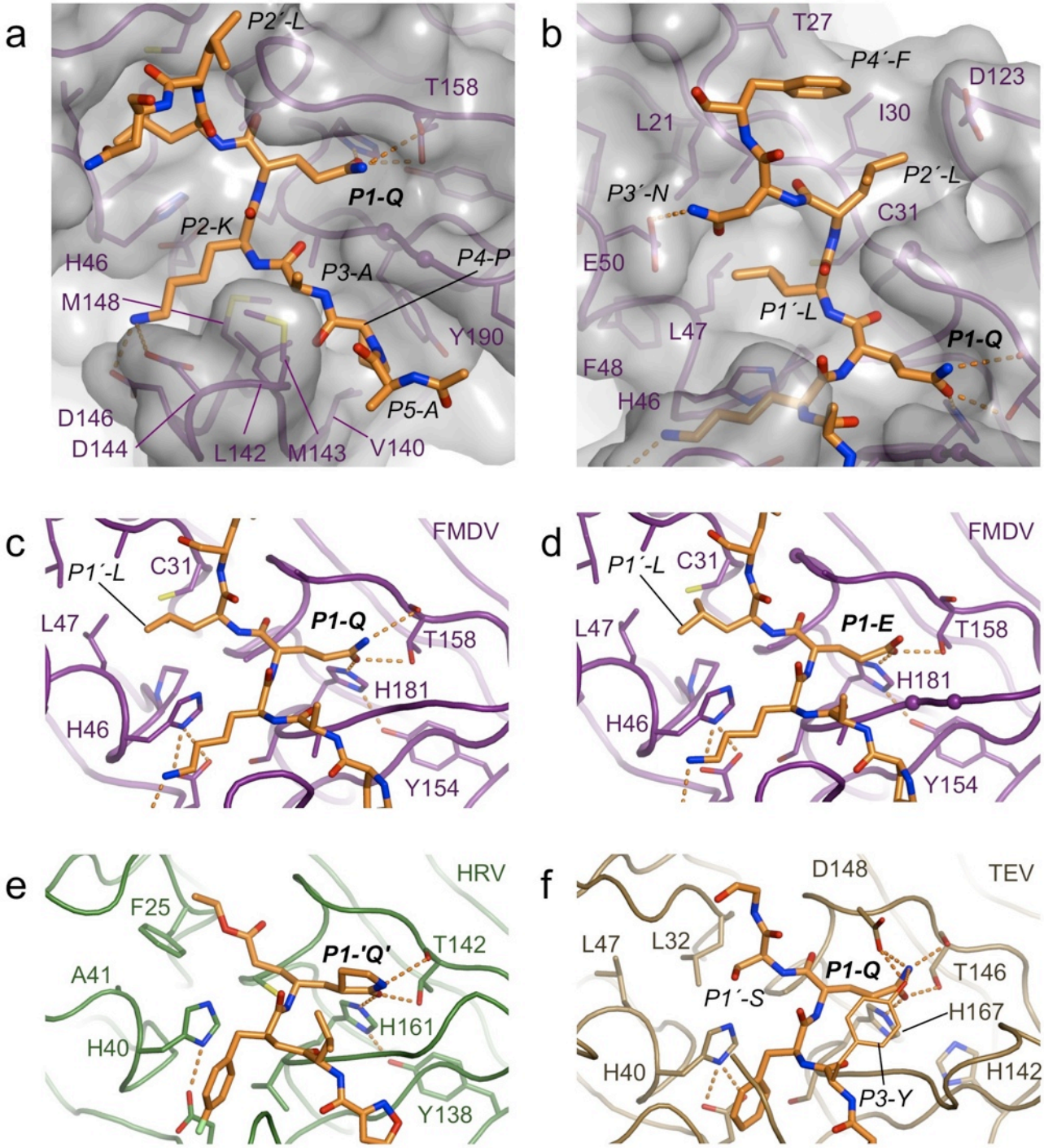

Figure 2: Structural details of peptide recognition by FMDV 3C^{pro}. (a) Close-up view of the binding of the P5-P1 residues from the VP1-2A peptide. The protease backbone is depicted as a smooth ribbon, covered by a semi-transparent grey Van der Waals surface; selected side-chains are shown. (b) Close-up view of the binding of the P1´-P4´ residues from the VP1-2A peptide. Detailed views of the P1-P1´ interactions for (c) FMDV 3C^{pro} complexed with VP1-2A and (d) FMDV 3C^{pro} complexed with VP1-2Am. The two hydrogen bonds made by OE1 from the P1-Glu side chain to Thr 158 and His 181 are shown as dotted lines; atom OE2 from the P1-Glu side chain is too distant from Thr 158 to form a hydrogen bond. (e) HRV 3C^{pro} complexed irreversibly with a peptide-like inhibitor[25]. (f) TEV NIA 3C-like protease complexed with a P7-P3´ peptide[28].

cleavage [8]. The origin of this discrepancy is unknown but the structural results are consistent with the more recent findings that the P4´ residue is unlikely to contribute significantly to substrate specificity (see below).

Structure determination

Recombinant type A10$_{61}$ FMDV 3C protease, inactivated by mutation of the active site Cys to Ala (C163A) and containing the C95K and C142L substitutions necessary for enhanced solubility[12], was purified from *E. coli* and co-crystallised with a five-fold molar excess of the decameric peptide, VP1-2A

(Materials and Methods). This peptide spans the P5-P5′ positions[22] and contains the sequence APAKQ|LLNFD from the VP1-2A junction in the polyprotein that was cut most rapidly in peptide cleavage assays[8]. The protease:peptide complex yielded crystals in space-group $P2_12_12_1$ that diffracted X-rays to 2.5 Å. The structure was determined by molecular replacement phasing using the structure of the free enzyme (PDB-ID 2j92; ref. 12) as a search model. There are two molecules in the asymmetric unit and the initial difference electron density map revealed clear density for the peptide bound to each molecule. The density was of high quality, consistent with full occupancy of the binding site, and readily allowed determination of the side-chain conformations for nine of the ten amino acids (P5-P4 ′) in the peptide. The electron density at the C-terminal end of the peptide was too weak to permit incorporation of the P5′-Asp residue in the refined model (Supplementary Fig. 1a). Atomic structures of the two 3C^{pro}-peptide complexes in the crystal were built using O[32] and refined with CNS[33] to yield a model with an R_{free} of 26.7% and excellent stereochemistry (Table 1).

An identical approach was applied to the preparation and structure determination of the complex of 3C^{pro} with the modified VP1-2Am peptide, which contains a Gln-to-Glu substitution at the P1 position. Although this peptide differs by only one amino acid from VP1-2A, the 3C^{pro}:VP1-2Am complex yielded crystals of a different space-group ($P2_1$) that diffracted to slightly lower resolution (2.7 Å). The dataset is only 76% complete but averaging across the four molecules in the asymmetric unit yielded a good quality electron density map (Supplementary Fig. 1b) that provided a clear indication of the bound conformation of residues P5-P4′ of the VP1-2Am peptide. The refined model has an R_{free} of 29.1% (Table 1).

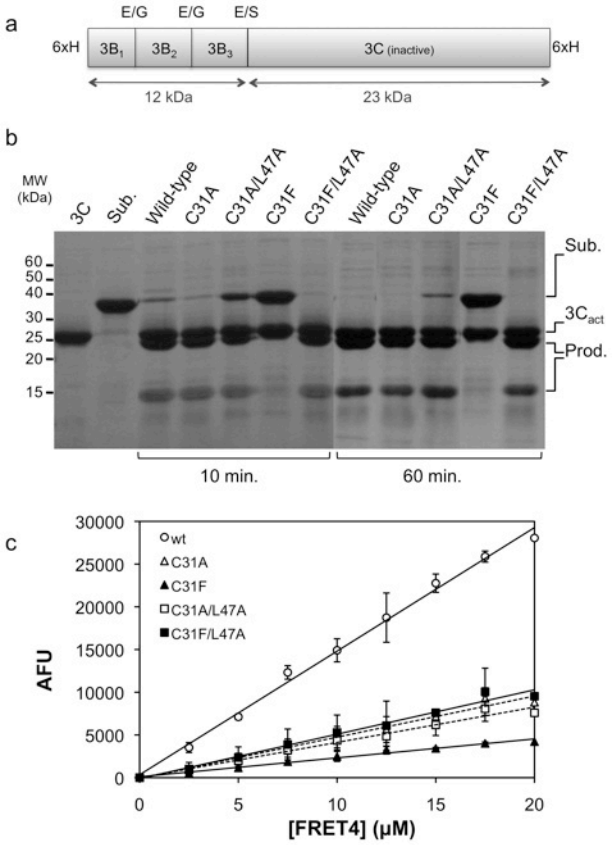

Figure 3: Mutagenic analysis of S1′ specificity. (a) Schematic diagram of the inactive polyprotein precursor used as a substrate in these cleavage assays which contains three cleavage junctions[44]. The P5-P5′ sequences of the three cleavage junctions in this polyprotein are $3B_1/3B_2$ – LPQQE|GPYAG; $3B_2/3B_3$ – PVVKE|GPYEG; $3B_3/3C$ – LIVTE|SGAPP. The sizes of the primary cleavage products are indicated. (b) SDS-PAGE analysis of polyprotein precursor digestion by FMDV 3C^{pro} S1′ mutants at 10 and 60 minutes. Labels on the right hand side indicate the substrate (Sub.), the active 3C^{pro} ($3C_{act}$) and the primary cleavage products (Prod.). (c) Comparative activity of FMDV 3C^{pro} S1′ mutants measured in the fluorescent peptide cleavage assay using the synthetic FRET4 substrate[31], which contains the VP1-2A cleavage junction (Materials and Methods). Data shown are the average fluorescence units from 3 experiments ±SEM.

Overview of the structure

The overall structures of the 3C^{pro}-peptide complexes obtained with VP2-2A and VP12Am are very similar to one another (Supplementary Fig. 2). There are differences in the backbone conformations of residues 105-109 at the C-terminal end of the polypeptide linking the two βbarrels of the enzyme, indicative of flexibility in this portion of the backbone. However, this is unlikely to impact peptide recognition since this part of the linker runs along the underside of the C-terminal β -barrel, opposite to the surface containing the peptide binding cleft.

When viewed with the inter-domain cleft aligned vertically (as in Fig. 1b,c), the peptide is observed to bind largely within a deep surface-groove that is oriented diagonally and intersects the cleft at the active site. Consequently residues P5-P1 on the amino-terminal side of the scissile bond mainly contact the C-terminal β-barrel, while residues P1′-P5′ interact primarily with the N-terminal β-barrel. The length of the recessed groove is sufficient to accommodate residues P4-P2′ of the peptide though residues outside this core are also in contact with the surface of the protease.

Conformational changes associated with binding

Comparison of the bound and free[12] forms for FMDV 3C^{pro} reveals several conformational changes that can be ascribed to peptide binding because they are observed for the six independent structures found in the asymmetric units of the crystals of both 3C^{pro}-peptide complexes, all of which have different packing environments in the crystal. These differences extend across both β-barrels (Fig. 1e; Supp. Movie 1). On the P5-P1 side the β-ribbon (residues 138-150) moves in to contact the peptide and there are adjustments in the backbone of the polypeptide that form the flanks of the S1 sub-site (β-strand E_2 and the C-terminal end of the C_2D_2 loop) (Fig. 1e); on the P1′-P5′ side of the peptide the most significant changes in backbone conformation occur in residues 47-53 and the nearby A_1-B_1 pair of β-strands (residues 18-31) that are in closest contact with the peptide. These two segments of polypeptide are altered due to a propagated series of side-chain movements initiated by the rotation of the side chain of Leu 47 that is necessary to accommodate the P1′-Leu residues of the peptide (see below).

Structural basis of peptide binding specificity

The extensive malleability of the peptide-binding surface allows the protease to form intimate contacts with the substrate along most of its length. In common with other trypsin-like proteases, there is a network of hydrogen bonds between the peptide and protease backbones that mimics the interactions between protein β- strands. In the case of the complex between FMDV 3C^{pro} and the VP1-2A peptide, there are nine such main-chain hydrogen bonds in total, extending from P4-Pro to P5′-Asp (Fig. 1e). These main-chain contacts are bolstered by hydrogen bonds and apolar contacts between the peptide side chains and the protease. We will consider each of these in detail.

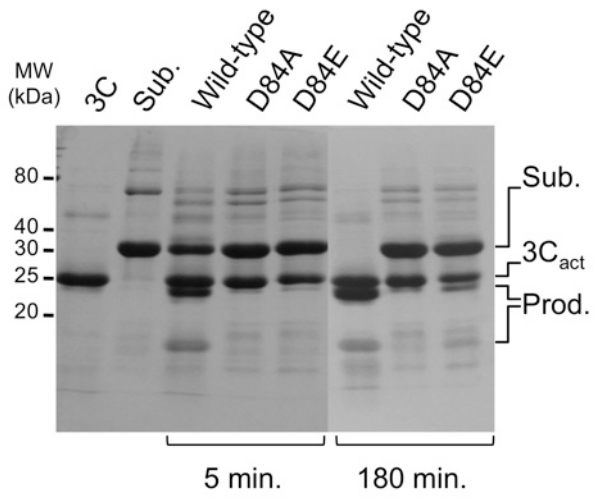

Figure 4: Mutagenic analysis of D84 from the catalytic triad. SDS-PAGE analysis of polyprotein precursor digestion by wild-type FMDV 3C^{pro}, and the D84A and D84E mutants at 5 and 180 minutes. The substrate is the same as depicted in Fig. 3a.

P5-Ala at the N-terminus of the peptide is largely solvent-exposed (Fig. 2a). The side chain points towards the hydrophobic side chain of Met 143 but is too far away (4.7 Å) to make contact. This lack of contact accounts for the finding that substitution by Arg, Leu or Pro at this position has only a modest effect on substrate cleavage, reducing the rate by two-fold at most (Fig. 1a).

P4-Pro, by contrast, is accommodated in a shallow, apolar depression that marks the beginning of the peptide-binding groove and is formed by the side chains of Leu 142 (Cys in the wild-type protein[12]), Val 140 and Tyr 190 (Fig. 2a). The P4-Pro side chain is not completely buried since one flank, containing the C_δ atom faces outward and is solvent-exposed. This part of the side chain is quite close to the carbonyl oxygen of Val 141 and side-chain hydroxyl of Tyr 190 (4.2 Å in each case). Intriguingly, mutation of the P4 residue to Val, Leu or Ile completely abrogated cleavage of the fluorescent substrate (Fig. 1a), consistent with a previous observation that an Ala substitution at this position also prevented cleavage[8]. These results suggest that, at least within the context of the VP1-2A peptide, there is a strict requirement for P4-Pro. Although the structure suggests that Ala and Val side chains, which are similar in size to Pro, should be accommodated in the S4 pocket, they may nevertheless affect the binding conformation sufficiently to prevent proper presentation of the scissile bond to the active site. This is a rather surprising result given the evident malleability of the protease. It is also unexpected since Ala, Val and Ile are observed at P4 in other FMDV polyprotein cleavage junctions, albeit within the context of different sequences [see Table II in [8]].

The side chain of P3-Ala points towards solvent but packs against Met 143 at the apical tip of the β-ribbon that alters its conformation on peptide binding to contact the P side of the substrate (Fig. 2a; Supp. Movie 1). This explains why, in common with other similar proteases, there is no strong preference for particular residues at this position in natural cleavage junctions[3]. In sequences cleaved by FMDV 3C^{pro} Val, Gln, Glu, His, Phe, Ser, Arg and Ala are found at P3, all of which could make some hydrophobic contact with the side chain of Met 143. Nevertheless, variation of this residue to Gln, Glu or Val within the context of the VP1-2A peptide reduces cleavage rates 5-10 fold, demonstrating that variation at the P3 position can affect cleavage (Fig. 1a). It may be that these larger side chains affect the positioning of the β-ribbon, which then has a knock-on effect on peptide interactions at other sub-sites.

The P2-Lys side chain inserts into the cleft between the β-ribbon and the body of the N-terminal β-barrel of the protease (Fig. 2a). On one side the Lys side chain primarily contacts the side chain of His 46 (the central residue of the catalytic triad), whereas on the other the aliphatic portion of the Lys contacts the apolar side chains of Leu 142 and Met 148. At the distal end of the pocket—which is open to solvent—there are salt bridges from the amine group at the tip of the Lys side chain to two acidic residues from the β-ribbon, Asp 144 (3.6 Å) and Asp 146 (2.8 Å) (Fig. 2a). Formation of the S2 pocket appears to be dependent on peptide binding since Leu 142, Asp144 and Asp 146 all adjust their positions in the presence of substrate (Fig. 1e). The salt bridges to the pair of Asp residues in the β-ribbon explains the strong preference for P2-Lys in natural substrates, (though it is not yet clear why this preference is strongest in substrates with P1-Gln[3]). Consistent with the acidic nature of the distal end of the S2 pocket, incorporation at P2 of norleucine (which is structurally similar to Lys but lacks the amine group) abrogates cleavage, whereas substitution by Arg or ornithine (both of which have a positive charge at the tip of the side chain) only modestly reduces the rate of peptide cleavage (Fig. 1a). Curiously, substitution by Thr also abrogates cleavage, even though this residue is found in other natural FMDV 3C^{pro} substrates[8]; it may be that Thr is tolerated at P2 only in the context of variation of the amino acids at other positions in the peptide substrate.

The side chain of P1–Gln is accommodated by small (0.7 Å) movements of the two backbone segments that form the flanks of the S1 pocket (residues 158-161 and 183-186) (Fig. 1e). The P1 side chain makes three hydrogen bonds to the pocket, two between the carbonyl group and the side chains of His 181 and Thr 158 (2.6-2.9 Å) and one from the amide group to the backbone carbonyl of Thr 158 (3.2-3.5 Å) (Fig. 2a,c). The pocket therefore displays good chemical complementarity to the P1-Gln side chain. However, peptide cleavage assays previously showed that incorporation of Glu at this position only reduces the cleavage rate by a factor of two[8], consistent with the common occurrence of P1-Glu in FMDV 3C^{pro} substrates[3]. To investigate this finding in more detail, we determined the crystal structure of 3C^{pro} bound to a modified VP1-2A peptide, in which P1-Gln is substituted by P1-Glu (VP1-2Am). The structure reveals that the P1-Glu side chain binds in a manner that is almost identical to that observed for P1-Gln in the VP1-2A peptide (Fig. 2c,d). One oxygen atom from the P1-Glu side-chain carboxylate (OE1) makes two hydrogen bonds (ranging in length from 2.4-2.8 Å over the four independent structures) to His 181 and Thr 158; but the other carboxylate oxygen (OE2) is more distant from the main-chain carbonyl oxygen of Thr 158 (3.2-3.7 Å) and — assuming that the side-chain carboxylate is deprotonated — cannot form a hydrogen bond. The fact that the OE2 oxygen is also exposed to solvent (Fig. 2d) may also attenuate any negative impact on binding by allowing access to positive counter-ions in the cytoplasm of infected cells.

It therefore appears that the primary interactions to the P1 side chain of the substrate are the two shorter hydrogen bonds made with the side chains of His 181 and Thr 158. The longer separation between the carbonyl oxygen of Thr 158 and the P1-Gln amide or the P1-Glu carboxylate oxygen (OE2) is likely to reduce the impact of these groups on peptide binding, thus allowing FMDV 3C^{pro} to cleave substrates containing either type of residue in the P1 position. The importance of the hydrogen bonds to the side chains of His 181 and Thr 158 is underscored by the finding that incorporation of uncharged (norleucine; Nle), longer (adipic acid; Adi) or shorter (Asp) carboxylated side chains at P1 prevents cleavage of the substrate by FMDV 3C^{pro} (Fig. 1e).

The binding of the P1′-Leu side chain is unusual because it is accommodated in a pocket that forms only when the protease interacts with the peptide substrate (Fig. 2b). In the free enzyme Leu 47 packs against Cys 31 to form the floor of a shallow S1′ pocket but peptide binding was found to induce rotation of the side chain of Leu 47 towards the core of the N-terminal β-barrel, thereby creating a much deeper compartment to accommodate the peptide side chain (Fig. 1e). The largely apolar sides of the S1′ pocket are formed on one side by Pro 44, His 46, Leu 47 and the aliphatic flank of Glu 50 and by Ala 29 and Cys 31 on the other. The displacement of Leu 47 has significant knock-on effects, leading to displacement of Phe 48, Tyr 52, Leu 21, and Ile 55; there is also alteration of the main chain conformation of residues 4852 (Fig. 1e; Supp. Movie 1).

As noted previously[3], large hydrophobic side chains at the P1′ position are preferred in natural FMDV 3C^{pro} substrates containing P1-Gln. This correlation of P1 and P1′ amino acids seems to be necessary for efficient cleavage since substitution of P1′-Leu by Gly yielded a ten-fold reduction in cleavage rate, whereas introduction of Val or Cys at P1′ reduced the rate of cleavage only two-fold (Fig. 1a). Examination of the structure suggests that a P1′-Gly side chain would be too small even to make stabilising contacts with the shallow form of the S1′ pocket.

Since the bound conformations of VP1-2A (P1-Gln) and VP1-2Am (P1-Glu) peptides are very similar, it was no surprise to find that incorporation of P1′-Gly within the context of the VP1-2Am sequence also gave a ten-fold reduction in the rate of cleavage (Fig. 1a). However, these results cannot explain the observation that natural FMDV substrates with P1-Glu are most frequently observed to have Gly at P1′ [3]. We suggest that sequences beyond the residues on either side of the scissile bond are important in ensuring that it is presented optimally to the active site.

P2′-Leu binds at one end of the recessed peptide-binding groove (Fig. 1b, 2b). The side chain packs against Ala 160, Gly 161, Ile 30 and the C_β group of Asp 123 and against the side chain of P4′-Phe from the peptide, but is still only partially shielded from solvent (Fig. 2b). The interaction between the P2′ and P4′ side chains may not be replicated in other peptides since neither position is particularly well conserved in polyprotein junctions cleaved by 3C (ref. 34). The apolar nature of the S2′ binding pocket explains the general preference for P2′ residues with some hydrophobic functionality (Ser, Lys, Thr, Leu in P1-Gln substrates; Pro, Gly, Leu and Ile in P1-Glu substrates).

The P3′Asn side chain is almost completely solvent-exposed but is positioned to form a hydrogen bond with Glu 50 on the enzyme surface (Fig. 2b). However, there is little sequence conservation at this position in FMDV 3C^{pro} substrates and the most common alternative P3′ residues (Tyr, Ala, Ile) would not maintain this interaction. The exposed position of P3′Asn explains why an EDANS group can be added to an Asp side chain at this position in the FRET4 peptide substrate without compromising its ability to be cleaved by FMDV 3C^{pro} [31].

P4′-Phe is also largely solvent-exposed and primarily contacts a small apolar patch on the upper surface of the C-terminal β-barrel formed by the side chain of Ile 30 and the methyl group of Thr 27 (Fig. 2b). The hydrophobic nature of this patch explains the general preference for residues with apolar side chains at P4′ [3]. Consistent with this notion substitution of P4′-Phe by Arg, Pro or Ala, all of which have significant apolar features, only modestly reduced the rate of peptide cleavage (Fig. 1e).

The position of P5′-Asp is unknown since there is no electron density for this residue. It appears to make no stabilising contacts with the protein, in agreement with the observation that mutation to Ala at P5′ had no effect of the rate of peptide cleavage[8].

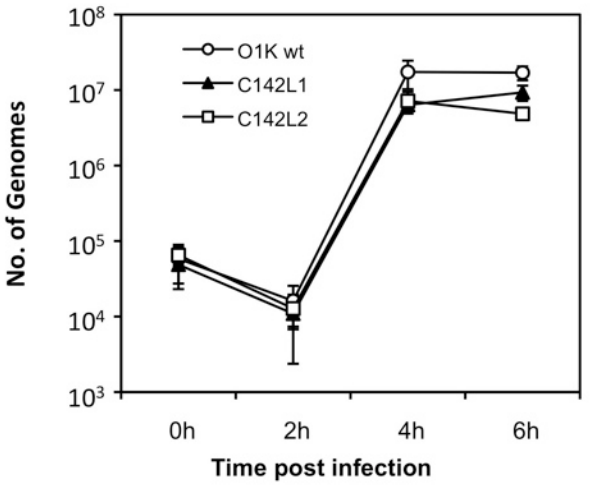

Figure 5: Infectivity of C142L mutants of O1K FMDV. Single step growth curves of wild-type O1K FMDV and two mutant viruses, both containing the C142L mutation in the βribbon of 3C^{pro}. The virus yield was determined by measuring the number of FMDV RNA genomes in a real-time RT-PCR assay (Materials and Methods).

Mutagenic analysis of the S1′ specificity pocket

As described above, the co-crystal structure of 3C^{pro} with the VP1-2A peptide revealed that binding of the peptide necessitated movement of Leu 47 to create a pocket deep enough to accommodate the P1′-Leu side chain (Fig. 1e). This S1′ pocket is the site of an interesting difference in specificity between FMDV 3C^{pro} on the one hand and 3C^{pro} from HRV and PV on the other. Whereas FMDV 3C^{pro} preferentially cleaves Gln-Xaa junctions, where Xaa is predominantly Leu, Ile or Thr[3], HRV and PV 3C proteases have a marked preference for cleavage at Gln-Gly junctions[15]. Comparison of the protease structures readily accounts for this difference since the Cys 31/Leu 47 residues that form the floor of the shallow S1′ pocket in the free form of FMDV 3C^{pro} are replaced by Phe 25/Ala 41 in 3C^{pro} from HRV [PDB-ID 1cqq; ref. 25] and PV [PDB-ID 1l1n; ref. 10] (Fig. 2c,e; Supp. Fig. 4). Examination of these structures suggests that steric hindrance would prevent the movement of Phe 25 that would be necessary to accommodate a large P1′ side chain.

We explored this idea by mutating the S1′ pocket on FMDV 3C^{pro} to make it resemble HRV 3C^{pro} and testing the effect on cleavage activity on a 3BC polyprotein substrate that contains Glu-Ser and Glu-Gly cleavage junctions, *i.e.* it has a small P1′ side chain (Fig. 3a; Materials and Methods). In this assay, the primary cleavage observed is at the Glu-Ser junction; further cleavage at the Glu-Gly junctions within $3B_1$-$3B_2$-$3B_3$ may be impeded by the low solubility of this fragment (Fig. 3a,b). Under the assay conditions used, wild-type FMDV 3C^{pro} cleaves over 95% of the substrate within 10 minutes. The single mutation C31F drastically reduced the ability of the protease to cleave this protein substrate; no cleavage was evident after a 1-hour incubation (Fig. 3b) and very partial cleavage was observed after 4 hours (Supp. Fig. 3). We estimate that the reduction in activity is approximately 200-fold. In contrast, mutation to the much smaller Ala side chain (C31A) had essentially no effect on the proteolytic activity of 3C^{pro} in this assay (Fig. 3b). The considerable reduction in the protease activity due to the C31F substitution is probably due to the steric strain that arises from close-packing of the large side chains of Phe 31 and Leu 47 in the S1′ binding pocket of the

mutant, which may have a knock-on effect on the position of His 46, a key component of the catalytic triad (compare Fig.s 2c and 2e; Supp. Fig. 4). This interpretation is strongly supported by the finding that the C31F/L47A double-mutation, which reduces the size of the side chain opposite Phe 31 and generates an S1′ pocket that resembles that found in HRV and PV 3C^pro, restores near wild-type cleavage activity (Fig. 3b). The C31A/L47A double-mutant is slightly impaired compared to the wild-type protease, perhaps because the P1′ residue is bound less tightly in the enlarged S1′ pocket.

We also investigated the impact of these S1′ mutations on cleavage of the fluorescent FRET4 substrate, which is based on the sequence of the VP1-2A peptide and contains a Gln-Leu cleavage junction; this substrate therefore places a large, hydrophobic side chain (P1′-Leu) in the S1′ pocket. As found previously, the C31F mutant showed the greatest impairment of cleavage activity, although the 7-fold reduction in cleavage rate compared to wild-type was much less than the ~200-fold reduction observed in the polyprotein cleavage assay (Fig. 3b). The precise reason for the difference in the magnitude of effect is not clear, but may relate to the different sequences that are being cleaved in the two experiments.

Strikingly, and in contrast to the result obtained with a substrate containing a small P1′ amino acid (Fig. 3b), the double mutation C31F/L47A did not rescue wild-type activity with the FRET4 substrate (though, as expected, the enzyme was slightly more active than the C31F single mutant) (Fig. 3c). Overall, these results are consistent with the structural data: the C31F/L47A double mutation would be predicted to make the S1′ pocket on FMDV 3C^pro resemble the inflexible, shallow depression found in the HRV enzyme (Supp. Fig. 4) which has a preference for substrates with a small P1′ residue.

Curiously the single C31A mutation reduced the rate of cleavage of the fluorescent VP1-2A peptide by about three-fold (Fig. 3c). This loss of activity possibly occurs because the P1′-Leu of the substrate was bound less snugly by the enzyme. As before the C31A/L47A double mutation caused only a very slight further reduction of the cleavage activity.

Mutagenic analysis of the catalytic Asp

The crystal structure of the 3C^pro-peptide complex reveals that the conformation of the catalytic triad is unchanged by peptide binding (Fig. 1e). In particular, it shows that Asp 84, the acidic member of the catalytic triad, maintains a hydrogen bond interaction with His 46, supporting the idea that this unusual class of trypsin-like cysteine proteases requires a full Cys-His-Asp triad for catalytic activity[8,14]. We tested this hypothesis by mutating Asp 84 (Fig. 4). The mutation D84E, which maintains a carboxylate side chain, reduced cleavage activity by about two orders of magnitude under our experimental conditions: whereas wild-type 3C^pro cleaved ~50% of the polyprotein in 5 minutes at 37°C, the D84E mutant cleaved <10% of the substrate after 180 minutes (Fig. 4). The mutation D84A was even more deleterious: there was no discernable cleavage of the substrate after 3 hours, consistent with a reduction in activity of at least three orders of magnitude.

These findings were confirmed in more quantitative assays using the fluorescent FRET4 peptide substrate (Supp. Fig. 5). Cleavage by the D84E mutant was about 200 times slower than by wild-type FMDV 3C^pro. Cleavage by the D84A mutant was at least 1000 times slower and was beneath the detection level of the assay.

Our results indicate that mutation of Asp 84 is even more deleterious to 3C^pro activity than was reported previously[35]. This apparent discrepancy is likely due to the greater sensitivity of our assay, which examined cleavage over a range of time points (Fig. 4). Our findings confirm the importance of Asp 84 for cleavage activity by FMDV 3C^pro and explain the strict conservation of this residue in all serotypes of FMDV[4].

Role of the β-ribbon in catalysis

The contacts that the side chain of Leu 142 in the β-ribbon makes with apolar features on P4-Pro and P2-Lys in the co-crystal structure explain the importance of this residue to catalytic activity (Fig. 1e, 2a)[12]. In FMDV 3C^pro this residue is strictly conserved as Cys[4], which is also apolar. Previously we mutated C142 to prevent aggregation of the protein due to formation of intermolecular disulphide bonds but found that substitution by a large hydrophobic side chain was necessary to preserve the catalytic activity of the protease[12,13]. Although slightly larger, Leu is a reasonable structural mimic of Cys, and the structure of the 3C^pro-peptide complex confirms our previous conclusion that the apolarity of C142 in the wild-type protein is necessary for its interaction with the P4 and P2 residues to ensure correct presentation of the polypeptide substrate to the active site[12]. Consistent with this idea, introduction of the C142L mutation into a type O1K FMDV had no significant effect on the infectivity of the virus in tissue culture (Fig. 5). This observation and the fact that the equivalent residue in HRV and PV 3C^pro is a leucine (Leu 127) nevertheless beg the question: why is Cys 142 strictly conserved in FMDV 3C^pro? We speculate that this may confer a selective advantage during infection of natural hosts by permitting inactivation of the protease upon cell lysis.

Discussion

An extensive, flexible interface for peptide recognition

We have determined the crystal structure of FMDV 3C^pro in complex with a specific peptide substrate, providing the first detailed view of enzyme-substrate interactions for this important group of picornavirus proteases. The mode of peptide binding is similar to that observed in HRV and HAV 3C proteases complexed with covalently attached peptide-like inhibitors[24-26] and with peptide complexes of other trypsin-like proteases[36] in that the peptide adopts a linear extended conformation that places the P1 side chain into the S1 specificity pocket within the C-terminal β-barrel, immediately adjacent to the catalytic triad. The mode of binding in FMDV 3C^pro involves the five mainchain-mainchain hydrogen bonds involving the P3-P1′ positions on the peptide that are conserved in trypsin-like proteases and appear to be necessary for proper positioning of the scissile bond in the active site[27].

However, the structure reveals that the enzyme-substrate interaction extends well outside this core region; all side chains from P4P4′ are involved to a greater or lesser extent in contacts with the surface of 3C^pro. Overall the structure of the complex is highly consistent with the results of experiments to probe the effect of variation of the side chain at different positions within the peptide substrate on cleavage rates, which suggest that the region P4-P2′ contributes most to peptide specificity. This is probably because these six residues occupy the deepest part of the surface groove that forms the peptide-binding cleft (Fig. 1c).

There are nevertheless some unexpected results from the cleavage assays that are not readily explained by the structure. For example, it is notable that, within the context of the VP1-2A cleavage junction sequence, conservative substitution of P4-Pro with residues such as Val or Ala that occur at this position in other junctions, leads to complete abrogation of peptide cleavage (Fig. 1a). The effect of these substitutions is all the more surprising given the evident flexibility displayed by the protease (Fig. 1e; Supp. Movie 1) but it is perhaps a reflection of the important role played by sites remote from the scissile bond in peptide cleavage efficiency[27,36].

The extensive interface of contact between the peptide and protease in FMDV 3C^{pro} exhibits similarities to that observed in the 3C-like TEV^{pro}, which was solved in complex with a peptide that spanned positions P7-P3´ [28] (Fig. 1c,d). Superposition of the two structures shows that the backbone geometry is similar over the common P4P3´ region. The structural similarity is closest for the core segment centred on the scissile bond (P2-P2´; root-mean-squared deviation over C_a = 0.14 Å), but there are significant structural deviations outside this region, dictated by the differing topologies of the peptide-binding cleft. In particular, TEV^{pro} provides a much more enclosed binding site for the P4-P3 residues due to the close apposition of the C-terminal β-ribbon with the E_2F_2 loop in the C-terminal β-barrel (Fig. 1d).

The FMDV 3C^{pro}-peptide interaction is also reminiscent of the extended interface observed in structures of specific protein *inhibitors* of trypsin and trypsin-like proteases such as chymotrypsin and collagenase[37-41]. These inhibitors are generally composed of a small stable domain that interacts with the target enzyme by inserting an extended internal loop, constrained at both ends, to the peptide-binding cleft of the target enzyme. The extent of the interaction varies from P3-P2´ in the complex of trypsin with pancreatic trypsin inhibitor[40] to P7-P4´ for ecotin bound to collagenase[38]. These inhibitors strongly mimic highly specific substrates but are usually cleaved extremely slowly because the rigidity of the enzyme-peptide interface prevents the conformational changes necessary to attain the tetrahedral intermediate at the scissile bond and the tightly packed interface prevents access of water molecules that would be necessary for the deacylation step of catalysis[42]. In contrast, in 3C proteases extensive sequence recognition must also be allied with sufficient flexibility to permit catalysis.

Although the residual flexibility in the 3C^{pro}-peptide complex that is necessary for catalysis is not detectable by crystallography, our results do reveal that structural adjustments are made across the peptide-binding surface upon substrate binding. Particularly notable are the movements of the β-ribbon to form the S2-S4 sub-sites, the strands flanking the S1 pocket and the large rotation of Leu 47 within the S1´ pocket to accommodate the large P1´ side chain (Fig. 1e). These observations are broadly consistent with previous NMR analyses of HRV 3C^{pro} which revealed flexibility throughout the enzyme that was attenuated by interactions between the protein and a peptide like inhibitor spanning P6-P1[24]. These marked conformational changes associated with peptide binding to FMDV 3C^{pro} are in contrast to the relatively rigid lock-and-key binding of some protein inhibitors to trypsin-like proteases[37,41] and underscore the importance of structural analysis of the peptide-bound form for obtaining a more complete picture of the substrate basis of cleavage specificity. This information is of particular relevance to inhibitor design though further structural analyses of FMDV 3C^{pro} bound to different peptide sequences will be needed to map out the full extent of structural changes that accompany substrate binding.

The conformational changes propagated by rotation of Leu 47 to accommodate the P1´ Leu in the FMDV 3C^{pro} substrate were unanticipated. Our structural and mutagenic analyses suggest that such side chain movements are very unlikely to occur in HRV or PV 3C^{pro} since the F25/A41 pair of residues that lie on either side of the pocket entrance (equivalent to C31/L47 in FMDV 3C^{pro}) do not have the flexibility to accommodate large P1´ side chains (Fig. 2c-e). This explains the strict requirement for small P1´ side chains — most often Gly — in substrates for 3C^{pro} from HRV and PV[15,21]. In contrast, HAV 3C^{pro}, like FMDV 3C^{pro}, is tolerant of larger P1´ residues (*e.g.* R, V, M)[21]. Since it has an M29/A45 pair of residues flanking the S1´ pocket, we suggest that the Met 29 side chain may have the ability to move to accommodate larger P1´ side chains.

S1 specificity

The crystal structures of FMDV 3C^{pro} in complex with the VP1-2A and VP1-2Am peptides show that P1-Gln or P1-Glu bind similarly within the S1 specificity pocket, both making hydrogen bonds from a side-chain oxygen atom to the side chains of Thr 158 and His 181; Tyr 154 also plays an important role in determining P1 specificity since it stabilises the orientation of His 181 (Fig. 2c,d). This structural arrangement accounts well for the observation that a Gln to Glu substitution at P1 within the VP1-2A peptide only modestly reduces peptide cleavage (Fig. 1a,e).

However, the bound conformation of P1-Gln in FMDV 3C^{pro} is also very similar to the conformation of the modified glutamine observed in the S1 pocket when the peptide-like inhibitor AG7088 is bound to HRV 3C^{pro} [25]. Although the glutamine side chain was altered to incorporate a lactam ring, glutamine-specific hydrogen bonds were observed in S1. It is therefore difficult to understand why FMDV 3C^{pro} readily cleaves substrates with P1-Gln or P1-Glu, while HRV 3C^{pro} exhibits a strong preference for P1-Gln substrates[15,17,20]. The discrepancy is all the more remarkable since the residues primarily responsible for P1-Gln or Glu recognition in FMDV 3C^{pro} (Thr 158, Tyr 154, His 181) are conserved in the P1-Gln-specific HRV 3C^{pro} *and* in the P1-Glu-specific V8 protease from *Staphylococcus aureus*[43].

Given the close structural similarity between FMDV and HRV 3C^{pro} in the S1 pocket, why does HRV 3C^{pro} discriminate so strongly against P1-Glu? In the 3CL^{pro} from TEV the selectivity for P1-Gln is enforced by an interaction between the Gln side chain amide and the carboxylate of Asp 148 (Fig. 2f)[28]; clearly the presence of this negatively charged side chain strongly disfavours binding of substrates with P1-Glu. But HRV 3C^{pro} lacks an equivalent repulsive group (Fig. 2e) and it remains unclear how discrimination against P1-Glu substrates is achieved.

It may be worth considering the impact of remote sites on P1 selectivity in these enzymes. As noted previously[3], FMDV 3C^{pro} substrates with P1-Glu most commonly have a small residue at P1´ and are less likely to conserve Lys at P2. Perhaps the correlated amino acid variations at these and other positions have a positive impact on cleavage of P1-Glu substrates. Further exploration of this notion will benefit from structural analysis of a complex of FMDV 3C^{pro} with a natural P1-Glu substrate.

Materials and Methods

Expression and purification of FMDV 3C^{pro}: The original construct which expresses a C-terminally truncated, catalytically inactive form of the type A10 FMDV 3C protease that contains C95K, C142S and C163A substitutions (see Table 2 in [13]), was modified for co-crystallisation trials using Quikchange (Stratagene) to engineer an S142L mutation. This generates a form of 3C^{pro} that has wild-type binding activity but remains soluble at purified protein concentrations in excess of 10 mg/ml [12]. This modified construct was used to generate additional 3C^{pro} variants by the same technique to add mutations to the active site and S1´ sub-site. FMDV 3C proteins were produced in *E. coli* and purified essentially as reported previously[12,13], although the gel filtration step was omitted. The purified proteins were concentrated to 5-6 mg/mL in 50 mM HEPES, pH7.1, 400mM NaCl, 1mM βmercaptoethanol and stored in small aliquots at -80°C before use in protease cleavage assays.

A modified pET-FMDV3CXS construct[13,44], inactivated by introduction of the C163A mutation in 3C, was used to express the 35 kD fragment of the FMDV A10 polyprotein that corresponds to 3B1-3B2-3B3-3BC. The protein, which has a

non-cleavable C-terminal His-tag was produced in BL21 (DE3) *E. coli* and purified to about 95% homogeneity on TALON beads (BD Biosciences) using the same protocol as for the active 3C^{pro} mutants.

Peptide synthesis: The peptides for co-crystallisation (VP1/2A – APAKQLLNFD; VP1/2Am – APAKELLNFD), synthesised by standard Fmoc solid phase synthesis as described previously[8] with acetylation of the N-terminus and amidation of the C-terminus to block charges, were purified by reversed phase HPLC and sequences confirmed by mass spectroscopy. The FRET4 substrate (and sequence variants) used in peptide cleavage assays was prepared as reported[12,31].

Complex formation and crystallisation: 3C^{pro}-peptide complexes were prepared at a 1:5.5 molar ratio of enzyme to peptide since this has worked well for related proteases[28]. Typically 50 µL of 3C^{pro} at 17 mg/ml protein in 100 mM HEPES, pH 7, 400 mM NaCl, 1 mM EDTA, 2 mM β-mercaptoethanol, 0.01% (w/v) sodium azide was mixed with 7 µL of 30 mM peptide dissolved in the same buffer, which yielded a final protein concentration = 14.9 mg/mL. The complex was incubated with rotation at room temperature for 1 hour and used immediately in sitting drop vapour diffusion crystallisation trials. Optimised crystals of 3C^{pro} bound to APAKQLLNFD were obtained by mixing 1 µL of complex with 3 µL taken from a 1 mL reservoir composed of 40-42.5% PEG 400, 0.2 M $LiSO_4$, 0.1 M Tris, pH 8.0. Similar conditions were used to crystallise the complex with APAKELLNFD peptide: 41-43% PEG 400, 0.2 M $LiSO_4$, 0.1 M Tris, pH 8.0.

Crystals were soaked for a few seconds in mother liquor that incorporated 20% (v/v) glycerol and flash-cooled on beamlines ID23-2 and ID14-2 at the ESRF in a stream of N_2 at 100 K. Diffraction data were processed with MOSFLM and scaled using SCALA from the CCP4 suite of programs[45]. The data for the 3C^{pro}:VP1-2A complex crystals were phased with PHASER (version 1.3.2)[46] using the unliganded structure of 3C^{pro} (PDB 2j92; ref. 12) as a search model after removal of the most mobile surface loops (residues 74-80 and 138-150). This procedure located two molecules in the asymmetric unit with an overall log likelihood gain of 1319. The protease structure from this model was then used to solve the structure of the 3C^{pro}:VP1-2Am complex, again using PHASER[46]. In that case, four molecules were identified in the asymmetric unit; the overall log likelihood gain was 3981. Manual model adjustment and refinement of both models were performed with O[32] and CNS[47] respectively.

Polyprotein cleavage assays: The cleavage activity of TALON-purified 3C^{pro} mutants was assessed using a protolytically inactive form of FMDV strain $A10_{61}$ 3BC precursor as a substrate[13,44]. Working stocks of 3C^{pro} and the 3BC substrate (Fig. 3a) were prepared at 2 mg/ml in 50 mM HEPES, pH 7.1, 400 mM NaCl and 20 mM DTT. In each assay equal volumes of substrate and 3C^{pro} were mixed to give a final concentration of each of 1mg/ml and incubated at 37°C for varying times up to 17 hours. Digestion reactions were stopped by direct addition of 5 µL of 2 × SDS-sample buffer to 5 µL of the reaction mixture, immediately followed by heating at 95°C for 2 min.

Fluorescent peptide cleavage assays: Assays were performed in 96 well plates essentially as described previously[12] with minor modifications. 50-100 µL of varying concentrations of the FRET4 fluorogenic substrate[31] was added to an equal volume of enzyme. Final enzyme concentrations were typically 1-2 µM (Wild-type), 5 µM (C31A, C31F, C31A/L47A and C31F/L47A mutants) or 10 µM (D84A and D84E mutants). Reactions were performed in triplicate at 37°C in 100 mM NaH_2PO_4/Na_2HPO_4, pH 7.4, 1 mM ethylenediaminetetraacetic acid, 1 mM Tris(2-Carboxyethyl)-Phosphine HCl and 5% glycerol. Relative hydrolysis rates were determined by monitoring fluorescence at 2 min intervals for 20-60 min in a Cytofluor microplate reader or a Molecular Devices SpectraMax M2^e. The excitation wavelength used was 335 nm and emission was measured at 460 nm. Initial hydrolysis rates were recorded (typically from 0-20 minutes) for each substrate concentration and specificity constants calculated by fitting to the Michaelis-Menten equation.

Infectivity assays: The generation of the C142L sequence change within the whole virus (type O1K) was achieved by overlap PCR using the pT7S3 infectious copy cDNA plasmid[48] as a template using the flanking primers 3AEcofor (AGGCAGCAATT*GAATTC*TTTGA) and 3CPstrev (CGTTGCCTC*CTGCAG*AGTGA) plus the degenerate mutagenic oligonucleotides 3CmutC142Lfor (ACTTACAAGGACATTGTGGTTCTNATGGACGGAGACACCATG) and 3CmutC142Lrev (CCGTCCATNAGAACCACAATGTCCTTGTAAGT). Up to 4 different codons (CTN) for leucine (L) could have been generated to replace the cys (C) residue codon (TGC) in this procedure but just 2 were used. The mutant PCR product including the EcoRI (nt 5058) - Pst1 (nt 6209) region (numbered according to Accession no. X00871) was inserted into pCR-XL-TOPO vector (Invitrogen) and individual plasmids were sequenced. The EcoRI-PstI fragments containing the CTA codon (C142L1) and CTG codons (C142L2) were excised and reconstructed into pT7S3 via an intermediate plasmid containing the BamHI fragment (nt 2909- nt 7117). The full-length wt and mutant plasmids were linearized with HpaI and RNA transcripts were prepared using T7 RNA polymerase (T7 Megascript kit, Ambion). The transcripts were introduced into BHK cells by electroporation, essentially as described previously[49]. Complete cytopathic effect was apparent following overnight incubation. The rescued virus harvests were passaged once in BHK cells and then RNA was extracted using a viral RNA extraction kit (Qiagen). RT-PCR reactions, (+/-) the reverse transcriptase, were performed using the primers (3AEcofor and 3CPstrev, as above) for 25 cycles. The expected products were only observed in the presence of the RT, (this ensured that products were derived from the viral RNA and not from residual cDNA template), the amplicons were then sequenced, using the same primers, and had maintained the respective wt or mutant sequences as anticipated (data not shown).

A single step growth curve of the rescued viruses was performed within BHK cells which were infected with wt or mutant viruses, in parallel, and the cells were harvested at t = 0, 2, 4 and 6 h post infection directly into RLT buffer (Qiagen), the first stage of the RNA extraction procedure. FMDV RNA was quantified by a standard diagnostic real-time RT-PCR assay as described previously[50,51] using amounts of RNA and cDNA which ensured that both the cDNA synthesis and real time PCR were within the linear range of the assays. The numbers of viral genomes in equal aliquots of RNA were determined by reference to a dilution series of RNA transcripts.

Accession Numbers: Coordinates and structure factors have been deposited in the Protein Data Bank with accession numbers 2wv4 and 2wv5.

Acknowledgements

We would like to thank staff on beamlines ID23-2 and ID14-2 at the ESRF (Grenoble, France) for assistance with X-ray data collection. SC and RJL are grateful for grant support from the BBSRC. We also thank Preben Normann, Inge Nielsen and Tina Frederiksen of the National Veterinary Institute in Lindholm and Imperial College students Siew Lian Low and George Wong for excellent technical assistance. SK was supported by an EPSRC PhD studentship; NRR was funded by a Marie Curie Host Fellowship for Early Stage Research Training; TS was funded by a PhD studentship awarded by Imperial College.

References

1. Sutmoller, P., Barteling, S. S., Olascoaga, R. C. & Sumption, K. J. (2003). Control and eradication of foot-and-mouth disease. *Virus Res* **91**, 101-44.
2. Grubman, M. J. & Baxt, B. (2004). Foot-and-mouth disease. *Clin Microbiol Rev* **17**, 465-93.
3. Curry, S., Roqué-Rosell, N., Zunszain, P. A. & Leatherbarrow, R. J. (2007). Foot-and-mouth disease virus 3C protease: Recent structural and functional insights into an antiviral target. *Int J Biochem Cell Biol* **39**, 1-6.
4. Carrillo, C., Tulman, E. R., Delhon, G., Lu, Z., Carreno, A., Vagnozzi, A., Kutish, G. F. & Rock, D. L. (2005). Comparative genomics of foot-and-mouth disease virus. *J Virol* **79**, 6487-504.
5. Skern, T., Hampoelz, B., Guarné, A., Fita, I., Bergmann, E., Petersen, J. & James, M. N. G. (2002). Structure and function of picornavirus proteases. In *Molecular Biology of Picornaviruses* (Semler, B. L. & Wimmer, E., eds.), pp. 199-212. ASM Press, Washington DC.
6. Belsham, G. J. (2005). Translation and replication of FMDV RNA. *Curr Top Microbiol Immunol* **288**, 43-70.
7. Allaire, M., Chernaia, M. M., Malcolm, B. A. & James, M. N. (1994). Picornaviral 3C cysteine proteinases have a fold similar to chymotrypsin-like serine proteinases. *Nature* **369**, 72-6.
8. Birtley, J. R., Knox, S. R., Jaulent, A. M., Brick, P., Leatherbarrow, R. J. & Curry, S. (2005). Crystal Structure of Foot-and-Mouth Disease Virus 3C Protease: New Insights into Catalytic Mechanism and Cleavage Specificity. *J Biol Chem* **280**, 11520-7.
9. Matthews, D. A., Smith, W. W., Ferre, R. A., Condon, B., Budahazi, G., Sisson, W., Villafranca, J. E., Janson, C. A., McElroy, H. E., Gribskov, C. L. & Worland, S. (1994). Structure of human rhinovirus 3C protease reveals a trypsin-like polypeptide fold, RNA-binding site, and means for cleaving precursor polyprotein. *Cell* **77**, 761-71.
10. Mosimann, S. C., Cherney, M. M., Sia, S., Plotch, S. & James, M. N. (1997). Refined X-ray crystallographic structure of the poliovirus 3C gene product. *J Mol Biol* **273**, 1032-47.
11. Lee, C. C., Kuo, C. J., Ko, T. P., Hsu, M. F., Tsui, Y. C., Chang, S. C., Yang, S., Chen, S. J., Chen, H. C., Hsu, M. C., Shih, S. R., Liang, P. H. & Wang, A. H. (2009). Structural basis of inhibition specificities of 3C and 3C-like proteases by zinc-coordinating and peptidomimetic compounds. *J. Biol. Chem.* **284**, 7646-55.
12. Sweeney, T. R., Roqué-Rosell, N., Birtley, J. R., Leatherbarrow, R. J. & Curry, S. (2007). Structural and mutagenic analysis of foot-and-mouth disease virus 3C protease reveals the role of the beta-ribbon in proteolysis. *J Virol* **81**, 115-24.
13. Birtley, J. R. & Curry, S. (2005). Crystallization of foot-and-mouth disease virus 3C protease: surface mutagenesis and a novel crystal-optimization strategy. *Acta Crystallogr D Biol Crystallogr* **61**, 646-50.
14. Yin, J., Bergmann, E. M., Cherney, M. M., Lall, M. S., Jain, R. P., Vederas, J. C. & James, M. N. (2005). Dual modes of modification of hepatitis A virus 3C protease by a serine-derived beta-lactone: selective crystallization and formation of a functional catalytic triad in the active site. *J Mol Biol* **354**, 854-71.
15. Blom, N., Hansen, J., Blaas, D. & Brunak, S. (1996). Cleavage site analysis in picornaviral polyproteins: discovering cellular targets by neural networks. *Protein Sci* **5**, 2203-16.
16. Cordingley, M., Callahan, P., Sardana, V., Garsky, V. & Colonno, R. (1990). Substrate requirements of human rhinovirus 3C protease for peptide cleavage in vitro. *The Journal of biological chemistry* **265**, 9062-5.
17. Cordingley, M. G., Register, R. B., Callahan, P. L., Garsky, V. M. & Colonno, R. J. (1989). Cleavage of small peptides in vitro by human rhinovirus 14 3C protease expressed in Escherichia coli. *J Virol* **63**, 5037-45.
18. Jewell, D. A., Swietnicki, W., Dunn, B. M. & Malcolm, B. A. (1992). Hepatitis A virus 3C proteinase substrate specificity. *Biochemistry* **31**, 7862-9.
19. Pallai, P. V., Burkhardt, F., Skoog, M., Schreiner, K., Bax, P., Cohen, K. A., Hansen, G., Palladino, D. E., Harris, K. S., Nicklin, M. J. & Wimmer, E. (1989). Cleavage of synthetic peptides by purified poliovirus 3C proteinase. *J Biol Chem* **264**, 9738-41.
20. Long, A. C., Orr, D. C., Cameron, J. M., Dunn, B. M. & Kay, J. (1989). A consensus sequence for substrate hydrolysis by rhinovirus 3C proteinase. *FEBS Lett* **258**, 75-8.
21. Seipelt, J., Guarne, A., Bergmann, E., James, M., Sommergruber, W., Fita, I. & Skern, T. (1999). The structures of picornaviral proteinases. *Virus Res* **62**, 159-68.
22. Schechter, I. & Berger, A. (1967). On the size of the active site in proteases. I. Papain. *Biochem Biophys Res Commun* **27**, 157-62.
23. Perona, J. J. & Craik, C. S. (1995). Structural basis of substrate specificity in the serine proteases. *Protein Sci* **4**, 337-60.
24. Bjorndahl, T. C., Andrew, L. C., Semenchenko, V. & Wishart, D. S. (2007). NMR solution structures of the apo and peptide-inhibited human rhinovirus 3C protease (Serotype 14): structural and dynamic comparison. *Biochemistry* **46**, 12945-58.
25. Matthews, D. A., Dragovich, P. S., Webber, S. E., Fuhrman, S. A., Patick, A. K., Zalman, L. S., Hendrickson, T. F., Love, R. A., Prins, T. J., Marakovits, J. T., Zhou, R., Tikhe, J., Ford, C. E., Meador, J. W., Ferre, R. A., Brown, E. L., Binford, S. L., Brothers, M. A., DeLisle, D. M. & Worland, S. T. (1999). Structure-assisted design of mechanism-based irreversible inhibitors of human rhinovirus 3C protease with potent antiviral activity against multiple rhinovirus serotypes. *Proc Natl Acad Sci U S A* **96**, 11000-7.
26. Yin, J., Cherney, M. M., Bergmann, E. M., Zhang, J., Huitema, C., Pettersson, H., Eltis, L. D., Vederas, J. C. & James, M. N. (2006). An episulfide cation (thiiranium ring) trapped in the active site of HAV 3C proteinase inactivated by peptide-based ketone inhibitors. *J Mol Biol* **361**, 673-86.
27. Perona, J. J. & Craik, C. S. (1997). Evolutionary divergence of substrate specificity within the chymotrypsin-like serine protease fold. *J. Biol. Chem.* **272**, 29987-90.
28. Phan, J., Zdanov, A., Evdokimov, A. G., Tropea, J. E., Peters, H. K., 3rd, Kapust, R. B., Li, M., Wlodawer, A. & Waugh, D. S. (2002). Structural basis for the substrate specificity of tobacco etch virus protease. *J Biol Chem* **277**, 50564-72.
29. Xue, X., Yu, H., Yang, H., Xue, F., Wu, Z., Shen, W., Li, J., Zhou, Z., Ding, Y., Zhao, Q., Zhang, X. C., Liao, M., Bartlam, M. & Rao, Z. (2008). Structures of two coronavirus main proteases: implications for substrate binding and antiviral drug design. *J. Virol.* **82**, 2515-27.
30. Bergmann, E. M., Cherney, M. M., McKendrick, J., Frormann, S., Luo, C., Malcolm, B. A., Vederas, J. C. & James, M. N. (1999). Crystal structure of an inhibitor

complex of the 3C proteinase from hepatitis A virus (HAV) and implications for the polyprotein processing in HAV. *Virology* **265**, 153-63.

31. Jaulent, A. M., Fahy, A. S., Knox, S. R., Birtley, J. R., Roque-Rosell, N., Curry, S. & Leatherbarrow, R. J. (2007). A continuous assay for foot-and-mouth disease virus 3C protease activity. *Anal Biochem* **368**, 130-7.
32. Jones, T. A., Zou, J. Y., Cowan, S. W. & Kjeldgaard, M. (1991). Improved methods for building protein models in electron density maps and the location of errors in these maps. *Acta Crystallogr.* **A47**, 110-119.
33. Brunger, A. T. (2007). Version 1.2 of the Crystallography and NMR system. *Nat Protoc* **2**, 2728-33.
34. Curry, S., Roqué-Rosell, N., Sweeney, T. R., Zunszain, P. A. & Leatherbarrow, R. J. (2007). Structural analysis of foot-and-mouth disease virus 3C protease: a viable target for antiviral drugs? *Biochem Soc Trans* **35**, 594-8.
35. Grubman, M. J., Zellner, M., Bablanian, G., Mason, P. W. & Piccone, M. E. (1995). Identification of the active-site residues of the 3C proteinase of foot-and-mouth disease virus. *Virology* **213**, 581-9.
36. Hedstrom, L. (2002). Serine protease mechanism and specificity. *Chem Rev* **102**, 4501-24.
37. Frigerio, F., Coda, A., Pugliese, L., Lionetti, C., Menegatti, E., Amiconi, G., Schnebli, H. P., Ascenzi, P. & Bolognesi, M. (1992). Crystal and molecular structure of the bovine alpha-chymotrypsin-eglin c complex at 2.0 A resolution. *J Mol Biol* **225**, 107-23.
38. Perona, J. J., Tsu, C. A., Craik, C. S. & Fletterick, R. J. (1997). Crystal structure of an ecotin-collagenase complex suggests a model for recognition and cleavage of the collagen triple helix. *Biochemistry* **36**, 5381-92.
39. Tsunogae, Y., Tanaka, I., Yamane, T., Kikkawa, J., Ashida, T., Ishikawa, C., Watanabe, K., Nakamura, S. & Takahashi, K. (1986). Structure of the trypsin-binding domain of Bowman-Birk type protease inhibitor and its interaction with trypsin. *Journal of Biochemistry* **100**, 1637-46.
40. Huber, R., Kukla, D., Bode, W., Schwager, P., Bartels, K., Deisenhofer, J. & Steigemann, W. (1974). Structure of the complex formed by bovine trypsin and bovine pancreatic trypsin inhibitor. II. Crystallographic refinement at 1.9 A resolution. *J Mol Biol* **89**, 73-101.
41. Fujinaga, M., Sielecki, A. R., Read, R. J., Ardelt, W., Laskowski, M. & James, M. N. (1987). Crystal and molecular structures of the complex of alpha-chymotrypsin with its inhibitor turkey ovomucoid third domain at 1.8 A resolution. *J Mol Biol* **195**, 397-418.
42. Laskowski, M. & Kato, I. (1980). Protein inhibitors of proteinases. *Annu. Rev. Biochem.* **49**, 593-626.
43. Prasad, L., Leduc, Y., Hayakawa, K. & Delbaere, L. T. (2004). The structure of a universally employed enzyme: V8 protease from Staphylococcus aureus. *Acta Crystallogr D Biol Crystallogr* **60**, 256-9.
44. Li, W., Ross-Smith, N., Proud, C. G. & Belsham, G. J. (2001). Cleavage of translation initiation factor 4AI (eIF4AI) but not eIF4AII by foot-and-mouth disease virus 3C protease: identification of the eIF4AI cleavage site. *FEBS Lett* **507**, 1-5.
45. Collaborative Computer Project No. 4. (1994). The CCP4 suite: programs for protein crystallography. *Acta Crystallogr. D* **50**, 760-763.
46. McCoy, A. J., Grosse-Kunstleve, R. W., Adams, P. D., Winn, M. D., Storoni, L. C. & Read, R. J. (2007). Phaser crystallographic software. *J Appl Crystallogr* **40**, 658-674.
47. Brünger, A. T., Adams, P. D., Clore, G. M., DeLano, W. L., Gros, P., Grosse-Kunstleve, R. W., Jiang, J. S., Kuszewski, J., Nilges, M., Pannu, N. S., Read, R. J., Rice, L. M., Simonson, T. & Warren, G. L. (1998). Crystallography & NMR system: A new software suite for macromolecular structure determination. *Acta Crystallogr.* **D54**, 905-921.
48. Ellard, F. M., Drew, J., Blakemore, W. E., Stuart, D. I. & King, A. M. (1999). Evidence for the role of His-142 of protein 1C in the acid-induced disassembly of foot-and-mouth disease virus capsids. *J Gen Virol* **80 (Pt 8)**, 1911-8.
49. Nayak, A., Goodfellow, I. G., Woolaway, K. E., Birtley, J., Curry, S. & Belsham, G. J. (2006). Role of RNA structure and RNA binding activity of foot-and-mouth disease virus 3C protein in VPg uridylylation and virus replication. *J Virol* **80**, 9865-75.
50. Belsham, G. J. & Normann, P. (2008). Dynamics of picornavirus RNA replication within infected cells. *J Gen Virol* **89**, 485-93.
51. Reid, S. M., Grierson, S. S., Ferris, N. P., Hutchings, G. H. & Alexandersen, S. (2003). Evaluation of automated RT-PCR to accelerate the laboratory diagnosis of foot-and-mouth disease virus. *J Virol Methods* **107**, 129-39.

Supplementary Information

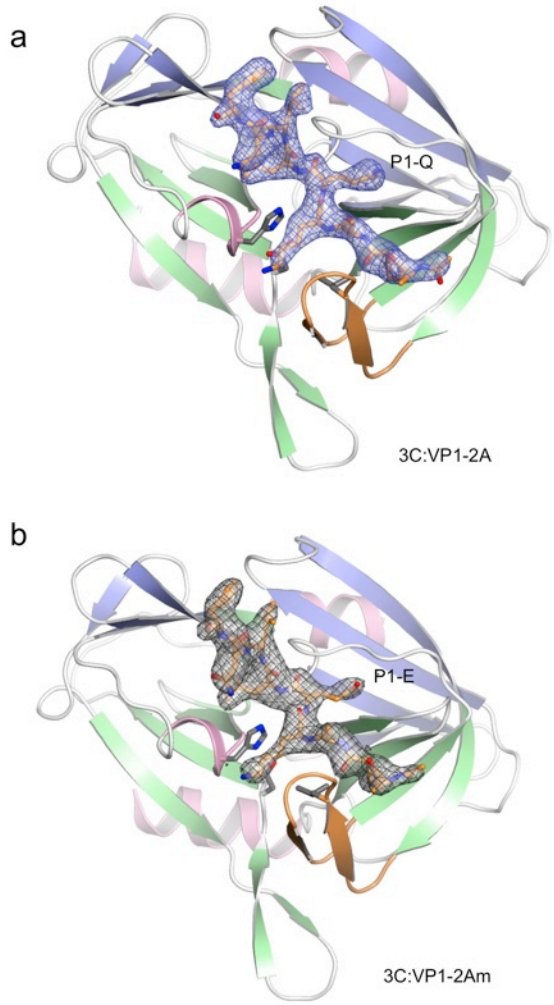

Supplementary Figure 1: Simulated annealing Fo-Fc omit maps contoured at 3σ for (a) 3C^{pro}:VP1-2A (2.5 Å resolution) and (b) 3C^{pro}:VP1-2Am (2.7 Å resolution).

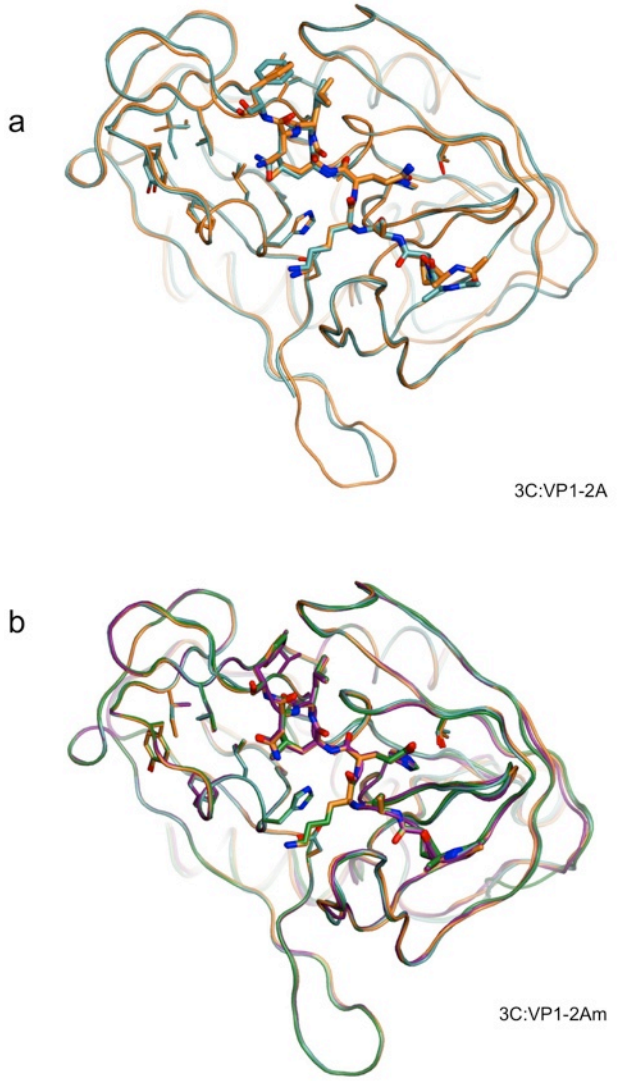

Supplementary Figure 2: Structural variation of co-crystal structures of 3C^{pro}-peptide complexes. (a) Superposition of the two structures of the 3C^{pro}:VP1-2A complex in the asymmetric unit of the $P2_12_12_1$ unit cell (Table 1). (b) Superposition of the four structures of the 3C^{pro}:VP1-2A complex in the asymmetric unit of the $P2_1$ unit cell (Table 1).

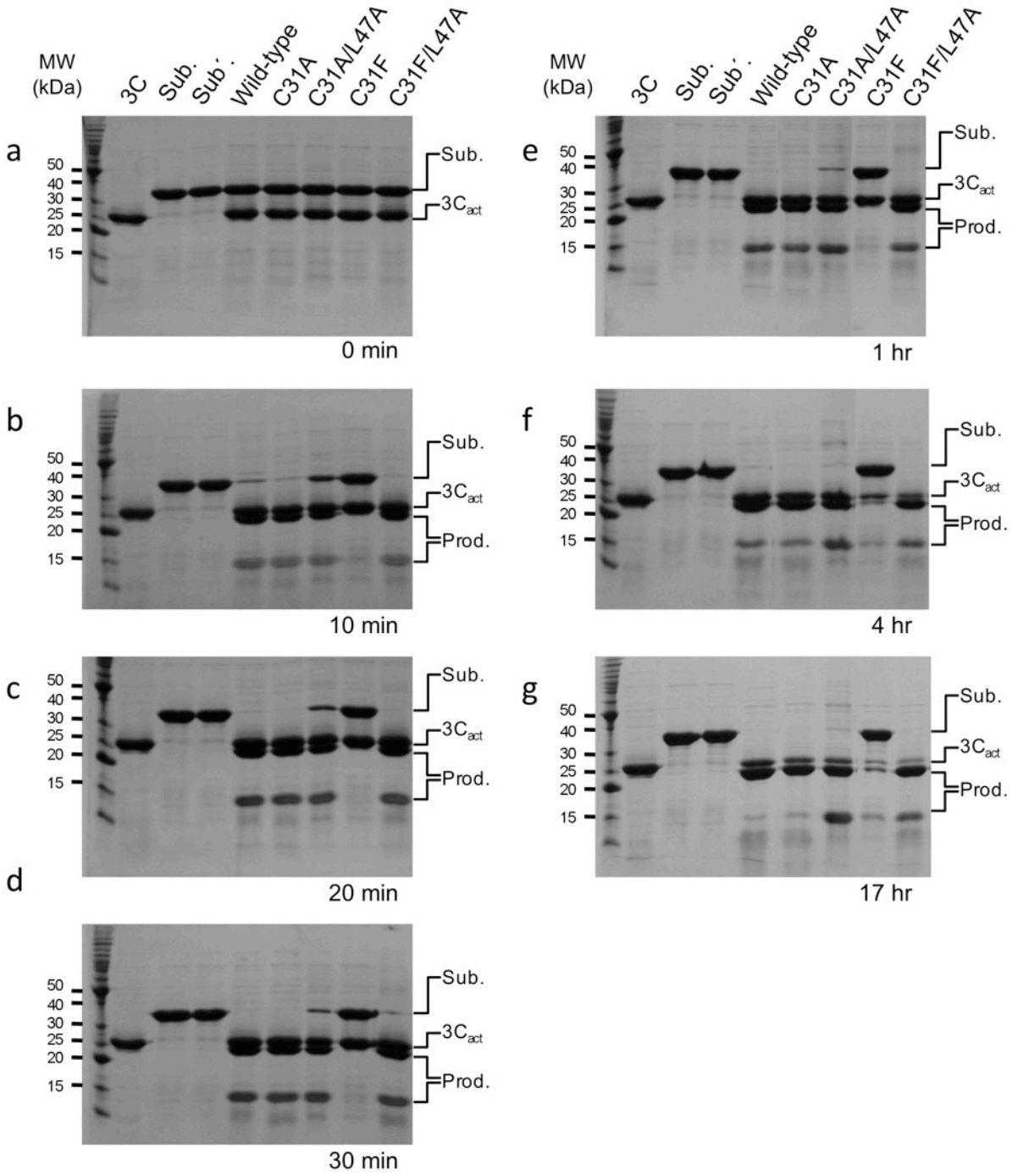

Supplementary Figure 3: Mutagenic analysis of S1´ specificity. SDS-PAGE analysis of polyprotein precursor digestion by FMDV 3C^{pro} mutants at (a) 0 min, (b) 10 min, (c) 20 min, (d) 30 min, (e) 1 hrs, (f) 4 hrs and (g) 17 hrs. The polyprotein precursor used is depicted in Fig. 3a. Labels on the right hand side indicate the substrate (Sub.), the active 3C^{pro} (3C$_{act}$) and the primary cleavage products (Prod.)

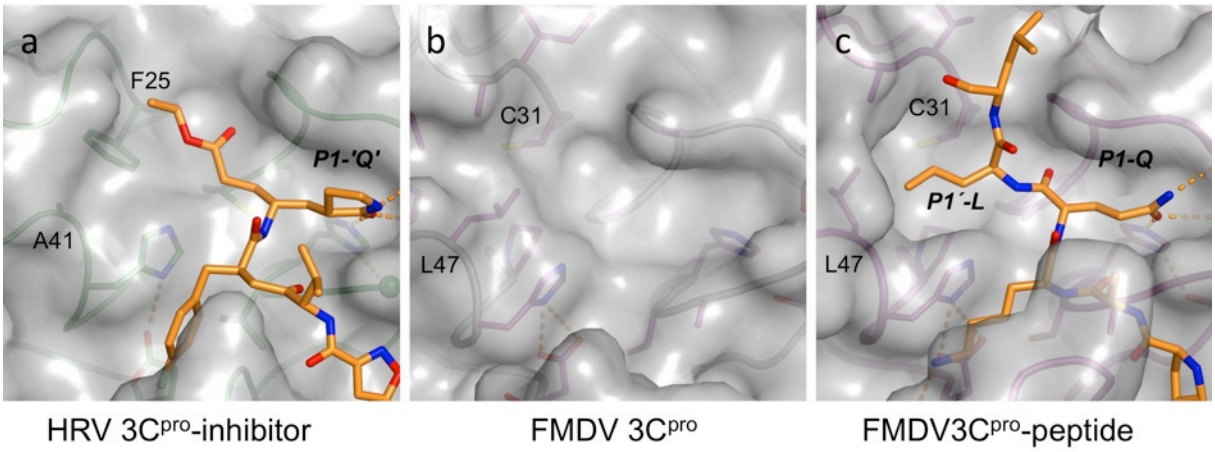

Supplementary Figure 4: Structural comparison of the S1´ binding pocket on FMDV and HRV 3C^{pro} (a) Complex of HRV 3C^{pro} and a peptide-like inhibitor[1] (PDB ID: 1cqq). The protein surface is coloured grey. The position of the cyclic glutamine side chain that occupies the P1 position in the inhibitor is labeled (P1-'Q'). (b) Structure of FMDV 3C^{pro} in the *absence* of a bound peptide[2] (PDB ID 2j92). (c) Complex of FMDV 3C^{pro} and the VP1-2A peptide (this work). The positions of the P1 and P1´ residues are indicated.

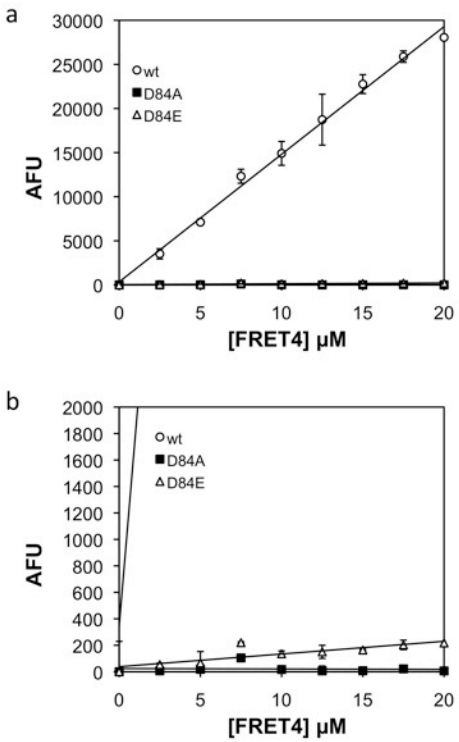

Supplementary Figure 5: Activity of D84 mutants of FMDV 3C^{pro} in fluorescent peptide cleavage assays. (a) Cleavage activity is observed as an increase in Arbitrary Fluorescent Units for a range of FRET4 substrate concentrations. (b) Same data as in panel (a) but rescaled on the vertical to show the difference between the D84E and D84A mutants. Note that at this scale, the first data point for the wild-type activity is off the graph.

Supplementary Movie 1:

Morph animation showing the conformational changes in FMDV 3C^{pro} upon peptide binding. Viewpoint is the same as Figure 1e. Further description of key features can be found in **the audio commentary** that accompanies the video.

The video can be viewed online at:

http://www.bio.ph.ic.ac.uk/~scurry/FMDV-3c-pep-morph.html

Supplementary References

1. Matthews, D. A., Dragovich, P. S., Webber, S. E., Fuhrman, S. A., Patick, A. K., Zalman, L. S., Hendrickson, T. F., Love, R. A., Prins, T. J., Marakovits, J. T., Zhou, R., Tikhe, J., Ford, C. E., Meador, J. W., Ferre, R. A., Brown, E. L., Binford, S. L., Brothers, M. A., DeLisle, D. M. & Worland, S. T. (1999). Structure-assisted design of mechanism-based irreversible inhibitors of human rhinovirus 3C protease with potent antiviral activity against multiple rhinovirus serotypes. *Proc Natl Acad Sci U S A* **96**, 11000-7.
2. Sweeney, T. R., Roqué-Rosell, N., Birtley, J. R., Leatherbarrow, R. J. & Curry, S. (2007). Structural and mutagenic analysis of foot-and-mouth disease virus 3C protease reveals the role of the beta-ribbon in proteolysis. *J Virol* **81**, 115-24.